Current Biology, Vol. 14, 763–775, May 4, 2004, ©2004 Elsevier Ltd. All rights reserved. DOI 10.1016/j.cub.2004.03.042

Microtubule Nucleation at Non-Spindle Pole Body Microtubule-Organizing Centers Requires Fission Yeast Centrosomin-Related Protein mod20p

Kenneth E. Sawin,[1,*] Paula C.C. Lourenco,[1,2] and Hilary A. Snaith[1]
[1]Wellcome Trust Centre for Cell Biology
University of Edinburgh
Edinburgh, EH9 3JR
United Kingdom

Summary

Background: Many types of differentiated eukaryotic cells display microtubule distributions consistent with nucleation from noncentrosomal intracellular microtubule organizing centers (MTOCs), although such structures remain poorly characterized. In fission yeast, two types of MTOCs exist in addition to the spindle pole body, the yeast centrosome equivalent. These are the equatorial MTOC, which nucleates microtubules from the cell division site at the end of mitosis, and interphase MTOCs, which nucleate microtubules from multiple sites near the cell nucleus during interphase.
Results: From an insertional mutagenesis screen we identified a novel gene, *mod20+*, which is required for microtubule nucleation from non-spindle pole body MTOCs in fission yeast. Mod20p is not required for intranuclear mitotic spindle assembly, although it is required for cytoplasmic astral microtubule growth during mitosis. Mod20p localizes to MTOCs throughout the cell cycle and is also dynamically distributed along microtubules themselves. We find that mod20p is required for the localization of components of the γ-tubulin complex to non-spindle pole body MTOCs and physically interacts with the γ-tubulin complex in vivo. Database searches reveal a family of eukaryotic proteins distantly related to mod20p; these are found in organisms ranging from fungi to mammals and include *Drosophila* centrosomin.
Conclusions: Mod20p appears to act by recruiting components of the γ-tubulin complex to non-spindle pole body MTOCs. The identification of mod20p-related proteins in higher eukaryotes suggests that this may represent a general mechanism for the organization of noncentrosomal MTOCs in eukaryotic cells.

Introduction

In many types of differentiated eukaryotic cells, including neurons, muscle, and epithelial cells, microtubules are not radially organized by the centrosome but rather are present in cell type-specific, noncentrosomal arrays with relatively stable microtubule minus ends. A variety of mechanisms has been proposed to account for the organization of these arrays; among these are centrosomal nucleation-and-release, microtubule breakage, and de novo assembly either in the cytoplasm or at specialized noncentrosomal sites [1, 2]. These different mechanisms are not exclusive of each other, and experimental support for each has been found in different systems (see [1, 2] for references). In general, however, relatively little is known about the molecular mechanisms regulating noncentrosomal microtubule organization, in part because some of the more striking examples, especially with regard to noncentrosomal microtubule nucleation sites, are found in specific tissues in vivo and not in standard cell culture systems [3–6]. Thus, what we do understand about the spatial control of microtubule organization in different cell types may represent only a fraction of the mechanistic diversity available to eukaryotic cells.

The fission yeast *Schizosaccharomyces pombe* has three different types of microtubule-organizing centers (MTOCs) during its normal mitotic cell cycle [7]. During mitosis, spindle and astral microtubules are nucleated from duplicated spindle pole bodies (SPBs), the centrosome equivalents [8]. At the end of mitosis, microtubules are nucleated from the cell division site by an equatorial MTOC (eMTOC) to form a post-anaphase array (PAA), which provides the initial array of interphase microtubules in the two daughter cells [7]. The eMTOCs contain γ-tubulin, and their formation depends on the actin cytoskeleton and contractile-ring formation [9, 10]. In the subsequent interphase, microtubule growth also occurs from additional, non-SPB microtubule-organizing centers, generally in the middle of cells, but the nature of these interphase MTOCs (iMTOCs) is not well understood [11–13].

Here we describe a novel fission yeast protein, mod20p, that is required for microtubule nucleation from the eMTOC and from iMTOCs but not from the SPB itself. Further analysis indicates that the role of mod20p in promoting this "noncentrosomal" microtubule nucleation is to bind and recruit the γ-tubulin complex to non-SPB MTOCs. We also find higher eukaryotic proteins with limited sequence similarity to mod20p, suggesting that this mode of microtubule organization may be conserved among eukaryotic cells.

Results

Aberrant Microtubules and Cell Shape in *mod20* Mutants

From an insertional mutagenesis screen [14] designed to identify nonessential genes regulating cytoskeleton and cell polarity in fission yeast, we isolated a mutant that exhibits a curved cell shape upon recovery from stationary phase, in particular when arrested during G2 of the cell cycle (Figures 1A and 1B; additional data not shown). This curved-cell phenotype is much less obvious during normal exponential growth (not shown), when microtubules are less important for cell polarity [15]. Sequencing of the genomic DNA flanking the insertion site identified a novel uncharacterized open reading frame identified as SPCC417.07c in the fission yeast

*Correspondence: ken.sawin@ed.ac.uk
[2] Present address: National CJD Surveillance Unit, Western General Hospital, Crewe Road, Edinburgh EH4 2XU, United Kingdom.

genome (http://www.sanger.ac.uk/Projects/S_pombe/); we have called this open reading frame *mod20+* (morphology defective 20). Deletion of the entire *mod20+* open reading frame (*mod20Δ*) produced a viable strain with the same phenotype as the original insertion mutant and was used for all subsequent analysis.

mod20+ encodes a predicted 1115 amino acid protein (mod20p) with extensive predicted coiled-coil regions and similarity to *Aspergillus nidulans* apsB [16] (see below and also Experimental Procedures). Because one of the phenotypes of *apsB* mutants is a nuclear-displacement defect, we examined nuclear positioning in *mod20Δ* mutants. Although wild-type fission yeast cells were able to maintain the nucleus in the middle of the cell, *mod20Δ* cells were not (Figure 1C). Because nuclear positioning in fission yeast depends on the microtubule cytoskeleton [12], we examined microtubule organization in *mod20Δ* mutants by immunofluorescence. In fission yeast, interphase microtubules are highly dynamic, and what appears to be a "single microtubule" at the light-microscopic level is in fact a bundle of between approximately four and seven microtubules [11–13]. In wild-type interphase cells, three or four of these bundles are typically observed per cell, ending at cell tips (Figure 1D). By contrast, *mod20Δ* mutants showed a range of aberrant microtubule distributions, marked by fewer, thicker microtubule bundles, which often curved around the cell tips (Figure 1E). We also found that the curved-cell phenotype of *mod20Δ* mutants was at least partially suppressed when microtubules were depolymerized with the drug methyl-benzimidazolyl 2-carbamate (MBC) [15], suggesting that the aberrant microtubule distribution in *mod20Δ* cells is a cause rather than an effect of the morphological defects (data not shown). Taken together, these results suggest that the curved cell shape and nuclear displacement phenotypes of *mod20Δ* mutants are likely to be secondary consequences of a primary defect in microtubule organization.

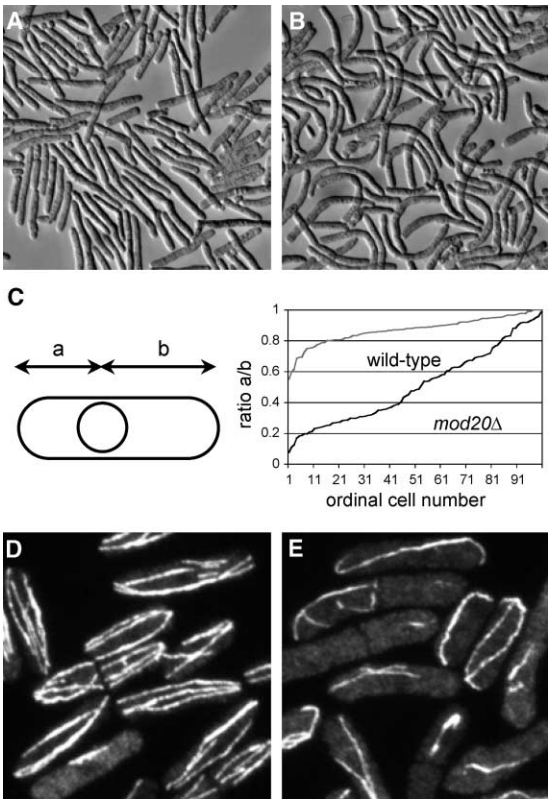

Figure 1. Cell Shape, Nuclear Displacement, and Microtubule Defects in *mod20Δ* Mutants

(A and B). Morphology of G2-arrested (A) *cdc25-22* and (B) *cdc25-22 mod20Δ* cells after 4 hr growth out of stationary phase.

(C) Measurements of nuclear eccentricity for 100 asynchronous wild-type and *mod20Δ* cells, in ascending order of the ratio a/b, where a is the shorter distance from the center of the nucleus to the cell tip, and b is the longer distance. a/b is greater than 0.5 in all wild-type cells but less than 0.5 in 50% of *mod20Δ* cells.

(D and E). Anti-tubulin immunofluorescence in asynchronous (D) wild-type and (E) *mod20Δ* cells.

mod20p Is at MTOCs

To establish a more mechanistic basis for the aberrant microtubule distribution of *mod20Δ* mutants, we determined the intracellular localization of mod20p by using both antibodies and GFP-fusion proteins. In living cells, mod20p-GFP expressed at native levels from the endogenous promoter was specifically localized to sites of microtubule nucleation: at the SPB during both interphase and mitosis and also at the eMTOC at the end of mitosis (Figure 2A and Movie 1, in the Supplemental Data available with this article online). During interphase we also found mod20-GFP localized to faint "satellite" particles that appeared to line up along microtubules and showed rapid back-and-forth linear movement (Figure 2A; see also Movie 2; additional data not shown). These satellites disappeared upon MBC treatment, whereas mod20p-GFP localization to the SPB and to the eMTOC persisted (Movie 3; additional data not shown). Immunofluorescent staining of endogenous mod20p with affinity-purified antibodies confirmed the observations made with mod20-GFP fusion proteins, including the localization of mod20p to the SPB and to satellite particles during interphase (Figures 2B and 2C) and to the SPB and the eMTOC during mitosis (Figures 2E–2G). In contrast to the localization of mod20p satellites to cytoplasmic interphase microtubules, virtually no mod20p was observed in association with the intranuclear mitotic spindle, apart from its localization to the SPB (Figures 2A, 2E, and 2F). In immunostained cells we also observed faint cytoplasmic particles of mod20p not associated with microtubules (Figures 2B and 2E–2G). These particles represent specific staining because they were not observed in *mod20Δ* cells treated with the same antibodies (Figure 2D). Although such particles were not apparent in live mod20-GFP-expressing cells (Figure 2A and Movies 1–3), they were observed in these same cells after fixation and staining (not shown); thus, it is not yet clear whether the cytoplasmic non-microtubule-associated mod20p particles are a fixation artifact or are simply too faint to be observed in live cells expressing mod20-GFP. In any case, collectively our results indicate that mod20p is strongly enriched at known MTOCs and also raise the possibility that interphase mod20p satellites could represent mobile nucleation complexes or iMTOCs (see below).

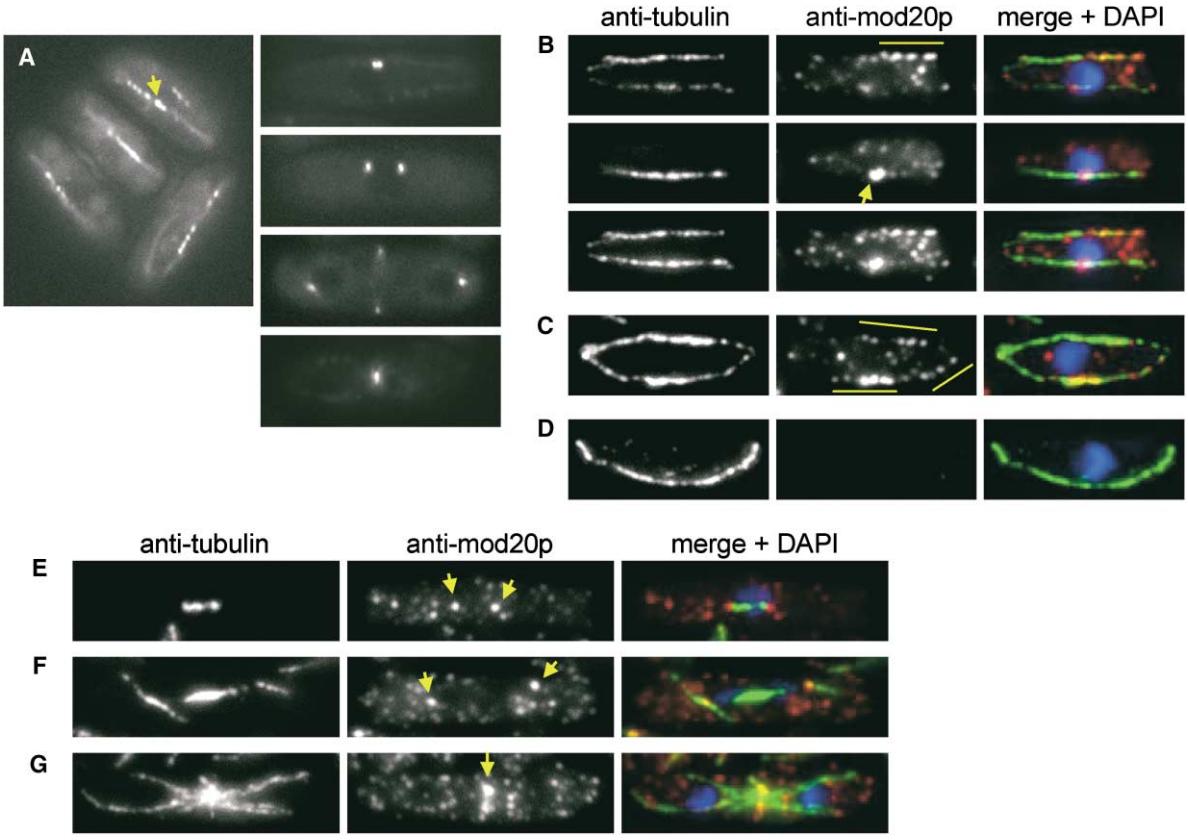

Figure 2. Localization of mod20p to Microtubule-Organizing Centers

(A) Unprocessed wide-field images of mod20-GFP localization along microtubules and at the spindle pole body (SPB) in interphase cells (left panel) and at the SPBs and the equatorial MTOC during cell division (right panels). An arrow indicates an in-focus interphase SPB. (B–G) Wide-field images of anti-tubulin and anti-mod20p staining in interphase and mitotic cells.

(B) Two Z sections of an interphase wild-type cell (top two rows) and a projection of all sections (bottom row). The bar indicates mod20p particles associated with cytoplasmic microtubules, and an arrow indicates the SPB.

(C) Projection of all sections of a different interphase wild-type cell, as in (B).

(D) Projection of all sections of an interphase *mod20*Δ cell. Note even faint anti-mod20p signal seen in (B) and (C) represents specific mod20p staining and not nonspecific background staining.

(E–G) Projection of all sections of a prometaphase/metaphase cell (E), an anaphase cell (F), and a postmitotic cell with a postanaphase microtubule array (G). Note that although mod20p is enriched at mitotic SPBs (arrows in [E] and [F]) and at the postmitotic equatorial MTOC (arrow in [G]), it is not associated with the intranuclear mitotic spindle.

mod20p and De Novo Interphase Microtubule Nucleation

To determine whether mod20p plays a role in microtubule nucleation, we performed microtubule depolymerization-regrowth experiments in vivo [12, 17, 18] and observed microtubule distributions at fixed time points. Cold treatment for 30 min depolymerized essentially all microtubules in both wild-type and *mod20*Δ cells (Figures 3A and 3B). Within 1 min after returning wild-type cultures to warm medium, we observed nucleation of microtubules from multiple independent sites over the surface of the cell nucleus (Figure 3B; [12, 17]). In addition, in 31% of cells, we observed one or more microtubules to nucleate more distantly, in the cytoplasm (Figure 3B, arrows; n = 365 cells). Microtubules in wild-type cells grew quickly and reached steady-state lengths within 4–10 min after warming (Figures 3D and 3E).

By contrast, *mod20*Δ mutants showed remarkably feeble nucleation of microtubules after warming, with significant new microtubule growth occurring only after 10–20 min (Figures 3F–3K). Moreover, in contrast to the multiple independent nucleation sites seen in wild-type cells, microtubule regrowth in *mod20*Δ mutants occurred in the form of a lone bundle of microtubules that appeared to grow in opposite directions from a single point on the nuclear surface (Figures 3J and 3K, arrows). This point colocalized with the SPB marker sad1p [19] in 84 out of 87 cells (Figure 3N). After this crippled nucleation, the microtubule distribution in *mod20*Δ mutants approached steady state (i.e., for *mod20*Δ mutants) very slowly, only after 30–60 min (Figures 3L and 3M), suggesting that, once established, microtubule bundles in *mod20*Δ mutants may turn over less rapidly than in wild-type cells.

These results indicate that mod20p is required for new microtubule nucleation from non-SPB sites during

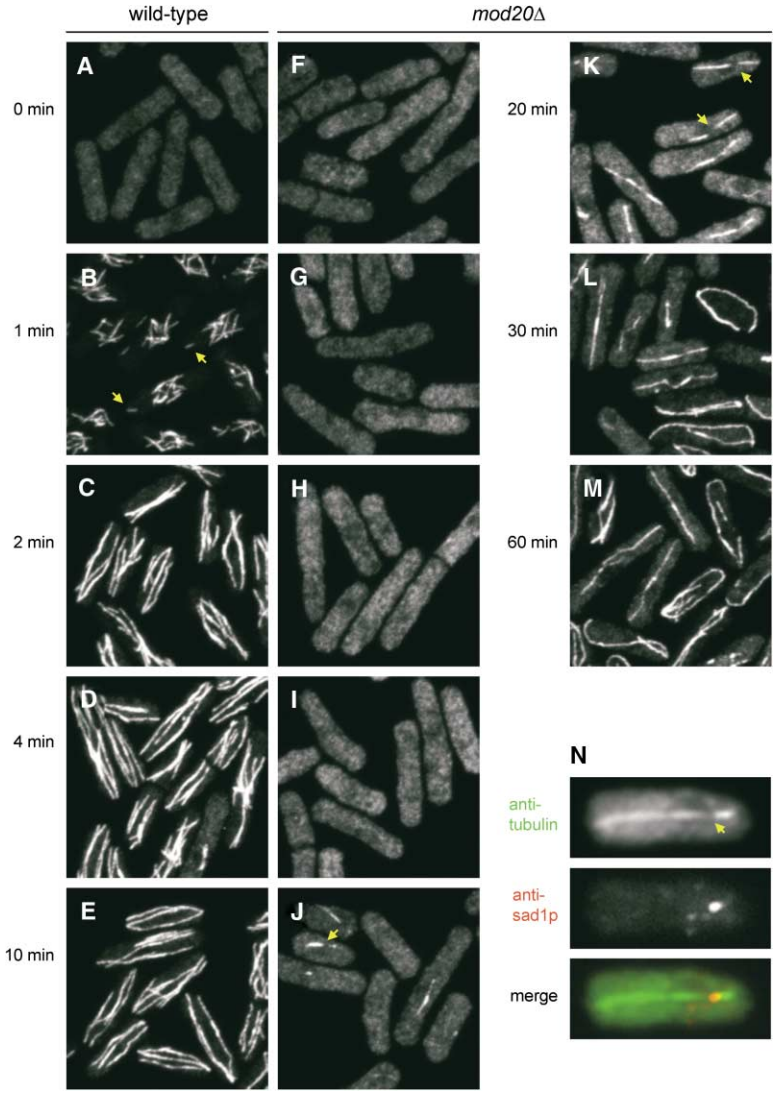

Figure 3. Mod20p Is Required for De Novo Microtubule Assembly from Non-Spindle Pole Body Sites

(A–M) Confocal images of anti-tubulin staining in *mod20*Δ and wild-type cells at different indicated times after recovery from a 30 min cold treatment to disrupt microtubules. Note that wild-type cells rapidly renucleate microtubules from multiple sites on the nuclear surface, as well as in the cytoplasm (arrows in [B]). Also note that the weak microtubule assembly observed in *mod20*Δ mutants generally occurs from a single site associated with the nucleus, which is slightly negatively stained (arrows in [J] and [K]).

(N) Wide-field images of anti-tubulin (top) and anti-sad1p (SPB marker; middle) staining in *mod20*Δ cells after 20 min recovery demonstrate that the site of microtubule nucleation in *mod20*Δ mutants is the SPB.

interphase. In conjunction with our data showing that mod20p is normally localized to MTOCs, this suggested that mod20p may play a direct role in nucleation. We therefore stained wild-type cells with anti-mod20p antibodies during cold treatment, prior to their warming and microtubule regrowth. Strikingly, we found that cold treatment leads to a strong, ectopic enrichment of mod20p particles to the nuclear surface, the site of future microtubule nucleation upon warming (Figure 4A). In addition, we found that in cells fixed after 1 min of regrowth, newly nucleated microtubules were associated with mod20p particles, not only on the nuclear surface but also at the more distant cytoplasmic nucleation sites that are found in many cells (Figures 4B and 4C; see also Figure 3B). These two results—the redistribution of mod20p to prospective but not yet active nucleation sites during cold treatment and the colocalization of mod20p particles with new microtubule ends in the cytoplasm—strongly suggest that mod20p acts directly at microtubule nucleation sites to promote nucleation and also support the notion that mod20p satellites in unperturbed interphase cells may be iMTOCs.

mod20p Is Not Essential for Mitotic Spindle Formation but Is Required for Astral Microtubules and for the Postanaphase Microtubule Array

During mitosis in fission yeast, the SPB nucleates intranuclear spindle microtubules and cytoplasmic astral microtubules, and in late mitosis, as the spindle disassembles, cytoplasmic microtubules are nucleated from an equatorial MTOC (eMTOC) at the cell division site and form a postanaphase microtubule array (PAA) [7, 9, 10]. The fact that *mod20*Δ strains are viable indicates that mod20p is not required for mitotic progression but does not address whether mod20p may still perform specific functions during mitosis. To investigate this, we performed spindle regrowth experiments during a synchronous mitotic metaphase arrest and release by using the reversible cold-sensitive β-tubulin mutant *nda3-km311* [20] in wild-type and *mod20*Δ backgrounds.

Upon release from metaphase arrest, rates of spindle regrowth and elongation were nearly identical in both *nda3* single mutants and *nda3 mod20*Δ double mutants (Figures 5B and 5E; Figure S1 in the Supplemental Data).

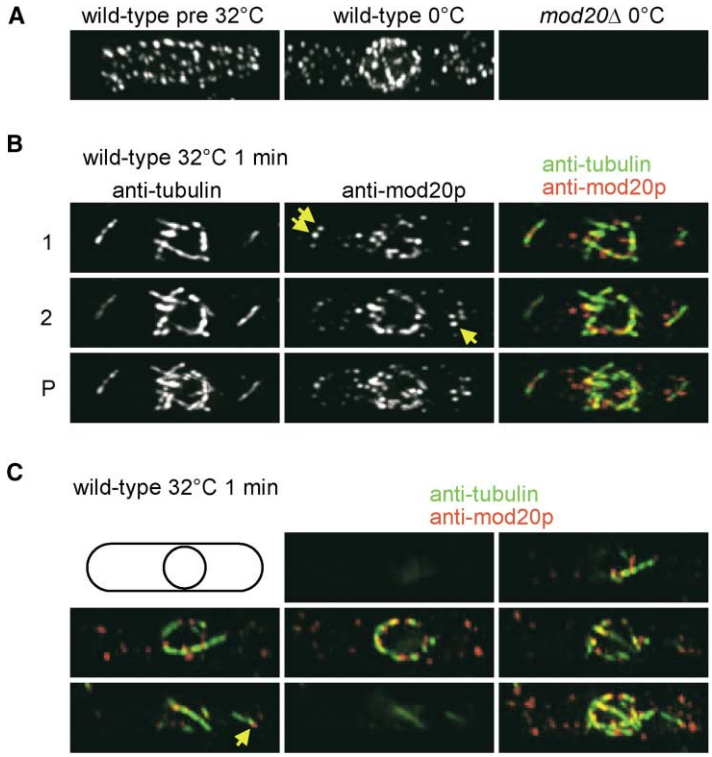

Figure 4. Mod20p Relocalizes to Prospective Microtubule Nucleation Sites during Cold Treatment and Is Directly Associated with Microtubule Ends Freely Nucleated in the Cytoplasm

(A) Anti-mod20p staining in wild-type cells before and during cold treatment. Mod20p is associated with microtubules before cold treatment but redistributes to the nuclear surface during cold treatment. Negative control *mod20*Δ cells show no staining.

(B) Anti-tubulin and anti-mod20p staining in a wild-type cell after 1 min recovery from cold treatment. Two different Z sections (1, 2) and a projection of all Z sections (P) are shown. Microtubules are specifically nucleated in proximity to mod20p; this is especially apparent for microtubules nucleated in the cytoplasm (arrows).

(C) Anti-tubulin and anti-mod20p staining in serial 0.4 um Z sections through a different wild-type cell after 1 min recovery from cold treatment. The final panel is a projection of all Z sections. Note the close association of mod20p with microtubule nucleation sites on the nuclear surface and in the cytoplasm (arrow). All panels are deconvolved wide-field images.

Progression into anaphase was also similar in the two strains, with 44% of *nda3* single mutants and 51% of *nda3 mod20*Δ double mutants passing into anaphase within 10 min after release (n = 230 cells for each strain; data not shown). This suggests that mod20p is unlikely to play a major role in mitotic spindle microtubule nucleation; accordingly, we did not observe any obvious defects in intranuclear spindle structure in *mod20*Δ mutants in these experiments (not shown). Interestingly, we did observe that *mod20*Δ mutants were strongly impaired in the growth of cytoplasmic astral microtubules (Figures 5B and 5E); 10 min after release, astral microtubules were seen in 73% of *nda3* single-mutant spindles but in only 8% of *nda3 mod20*Δ double-mutant spindles (n = 104 cells for each strain; data not shown); this defect was also observed in *mod20*Δ single mutants growing asynchronously (data not shown).

In order to confirm this cytological data, we also measured mitotic missegregation of a nonessential minichromosome [21] in *mod20*Δ mutants relative to wild-type cells and crossed *mod20*Δ mutants with several spindle checkpoint mutants [22]. Double mutants of *mod20*Δ in combination with *bub1*Δ, *bub3*Δ, *mad1*Δ, *mad2*Δ, *mad3*Δ, or *mph1*Δ were all viable and were obtained from crosses with expected Mendelian frequencies (data not shown), indicating that loss of mod20p does not activate the spindle checkpoint. Minichromosome loss rates in *mod20*Δ mutants were only mildly increased in relation to wild-type cells (approximately 6–8 times; data not shown). Taken together, these genetic data suggest that spindle mechanics are unlikely to be significantly impaired by loss of mod20p. The mechanistic basis for the small increase in chromosome loss rates is not yet clear but may be due to a combination of factors (see Discussion).

At later times after release from metaphase arrest, a more striking difference was observed between *nda3-km311* single-mutant cells and *nda3-km311 mod20*Δ double mutants. Although most *mod20*+ cells underwent spindle disassembly and PAA formation within 20 min after release (Figure 5C), PAAs never appeared in *mod20*Δ mutants (Figure 5E). In lieu of PAA formation, spindles persisted for slightly longer times, but interphase microtubules appeared in the next cell cycle with roughly similar kinetics in both strains (Figures 5F and 5G; Figure S1). To confirm that this complete absence of PAAs in *mod20*Δ mutants was not unique to mitotic arrest-and-release experiments, we also quantitated PAAs in asynchronous cultures. In wild-type cultures, 8% of cells contained PAAs, whereas 0% did so in *mod20*Δ cells (n = 500 cells for each strain; data not shown).

Microtubule Nucleation and Dynamics in *mod20*Δ Mutants at Steady State

The perturbation experiments described above suggest that mod20p is required for microtubule nucleation at non-SPB sites during both interphase and mitosis (i.e., at iMTOCs and at eMTOCs), as well as being required for cytoplasmic astral microtubules. To investigate cells growing at steady state, we examined microtubule dynamics in wild-type and *mod20*Δ cells expressing chromosomally integrated GFP fusions with atb2p, the minor α-tubulin in fission yeast [23]. Surprisingly, preliminary experiments indicated that GFP-atb2p strains routinely used for assays of microtubule dynamics in wild-type cells [14, 24, 25] significantly compromised microtubule integrity in *mod20*Δ mutants (Table S1). We minimized these defects by expressing GFP-atb2p at low levels

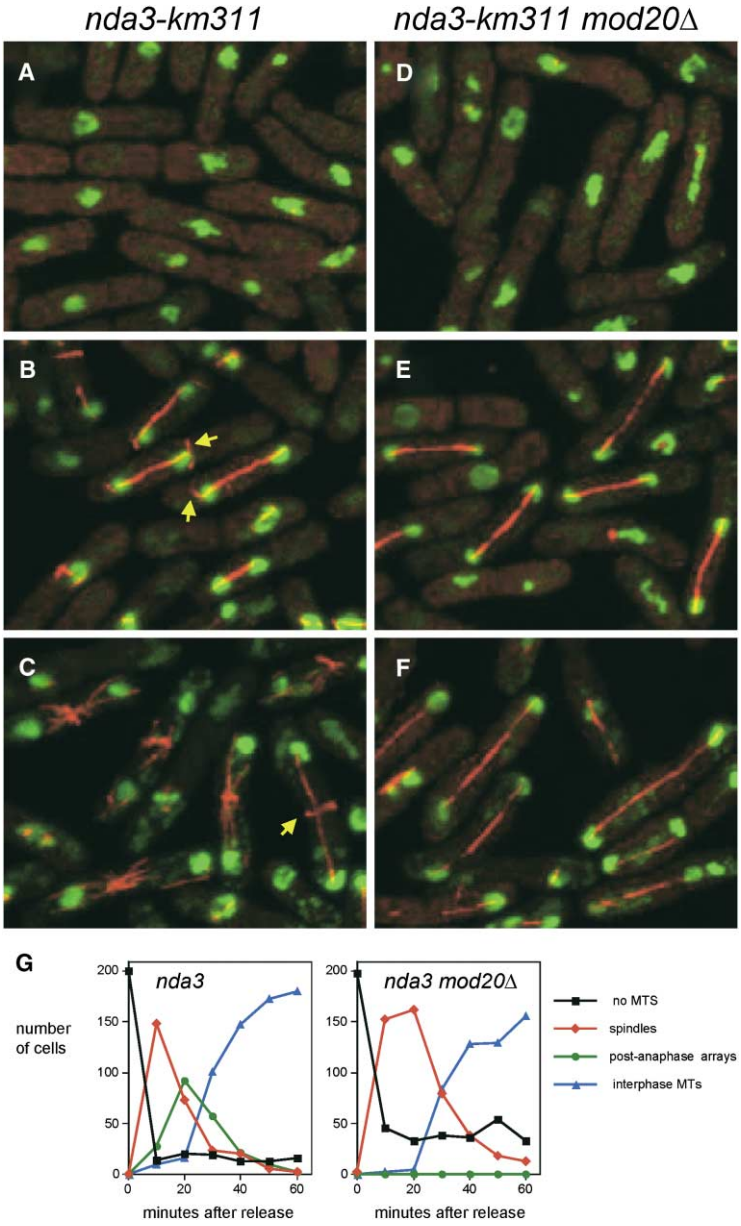

Figure 5. Mod20p Is Required for Astral Microtubules and for Postanaphase Microtubule Array Formation at the End of Mitosis

(A–F) Confocal anti-tubulin (red) and DAPI (green) staining of (A–C) *nda3-km311* and (D–F) *nda3-km311 mod20*Δ cells at 0 min (A and D), 10 min (B and E), and 20 min (C and F) after release from mitotic metaphase arrest. Arrows in (B) indicate astral microtubules, which are usually not observed in *mod20*Δ mutants. The arrow in (C) indicates PAA formation at an early stage relative to other cells in the panel.

(G) Evolution of microtubule arrays after release from metaphase arrest. Note the complete absence of PAAs in *mod20*Δ mutants.

from the *nmt81* promoter (Table S1), although imaging under these conditions was more challenging.

In cells expressing *nmt81*:GFP-atb2p, a high degree of variation in microtubule distribution and bundling was observed in *mod20*Δ mutants relative to wild-type cells; these observations were similar to those in fixed cells (data not shown). We focused our attention on microtubule nucleation. Over a total of 10 cell-hours, we did not observe any new microtubule nucleation in *mod20*Δ mutants, whereas in wild-type cells we observed nearly 300 likely nucleation events (Table 1; Movie 4). In addition, we found that in contrast to wild-type cells, in which microtubules reaching the cell tip usually pause and then initiate catastrophe and shrinking [11–13, 26], microtubule bundles reaching the cell tip in *mod20*Δ mutants often continued to grow around the tip and bend, sometimes sufficiently for the microtubule bundle to break into two distinct bundles (Figure 6; Movie 5). Such "bend-breakage" events were never observed in wild-type cells but occurred 32 times in *mod20*Δ mutants over a period of 10 cell-hours (Table 1).

The profound defects in microtubule nucleation seen in *mod20*Δ mutants raise the question as to how normal asynchronous *mod20*Δ cells generate interphase microtubules (see Figure 1). One possibility is that, at the end of mitosis, the SPB nucleates a small number of cytoplasmic microtubules that persist into the subsequent interphase; this population could also be augmented by bend-breakage events generating new microtubules. For technical reasons involving photobleaching and/or photodamage (not shown), we were unable to follow microtubules from anaphase into the next interphase in *mod20*Δ cells expressing *nmt81*:GFP-atb2p as a tubulin reporter. However, using slightly higher GFP-atb2p ex-

Table 1. Microtubule Nucleation and Breakage in Wild-Type and *mod20*Δ Cells

Strain	*nmt81:GFP-atb2*	*mod20*Δ *nmt81:GFP-atb2*
Number of cells observed	29	23
Total elapsed time	10 hr 26 min	10 hr 15 min
De novo microtubule nucleation events	114	0
Additional microtubule nucleation events	182	0
Microtubule bend-breakage events	0	32

We define "de novo" nucleation events as occuring away from existing microtubule bundles, whereas "additional" nucleation events occurred closer to existing bundles and may have been derived from pre-existing microtubule fragments.

pression levels (Table S1), we found that in a small number of cells (less than 10% of those observed), SPB-nucleated microtubules could break out of the cell nucleus at the end of mitosis and establish an independent existence in the cytoplasm, with very complicated dynamics involving bundling and bend-breakage (Movies 6 and 7). Although this was a low-frequency event, and although in most other cells the spindle simply disassembled with no additional SPB nucleation (data not shown), immunofluorescence of fixed cells expressing untagged atb2p also suggested that unusual modes of microtubule nucleation may occur in *mod20*Δ cells at the end of mitosis (Figure S2). Thus, in spite of incomplete resolution of this issue, as well as the caveats associated with making strong inferences from GFP-microtubule dynamics in *mod20*Δ mutant cells (see Discussion), our results are consistent with the notion that SPB-mediated microtubule nucleation is the ultimate source of interphase microtubules in *mod20*Δ mutants.

Interaction of mod20p with γ-Tubulin Complex

Microtubule nucleation in eukaryotic cells is thought to be directed primarily by the γ-tubulin ring complex, a multi-protein complex containing γ-tubulin and several other conserved proteins [27–29]. In fission yeast, γ-tubulin is found at SPBs throughout the cell cycle, as well as at eMTOCs during cell division [9, 30, 31]. To investigate whether mod20p might be required for the proper localization or function of the γ-tubulin complex, we stained *mod20*+ and *mod20*Δ cells in the *nda3* mitotic arrest-and-release experiment with antibodies to γ-tubulin. In postanaphase *mod20*+ cells, γ-tubulin was localized to the equator either as dots or as a faint equatorial ring, but in *mod20*Δ mutants, no equatorial γ-tubulin staining was observed, although γ-tubulin was still found at the SPB in *mod20*Δ mutants (Figure 7A). These results indicate that mod20p is required for γ-tubulin localization to the eMTOC, but not to the SPB.

To date, the γ-tubulin complex has not been observed at non-SPB microtubule nucleation sites during interphase [9, 30, 31]. We reasoned that the γ-tubulin complex proteins may be present at iMTOCs but at such low concentrations that they are difficult to detect above background. We therefore tried to visualize interphase non-SPB γ-tubulin complexes by fixing cells during cold treatment, when mod20p, and nearly all cytoplasmic microtubule-nucleating activity, is concentrated at the nuclear surface (see Figure 3). Wild-type and *mod20*Δ cells were costained with antibodies to mod20p and to an HA-tagged version of alp4p, a γ-tubulin complex core subunit [32]. In wild-type cells, we observed an accumulation of alp4-HA particles at the nuclear surface, but no such accumulation occurred in *mod20*Δ cells, although alp4-HA was still present at normal levels at the SPB (Figure 7B). This indicates that mod20p is important for γ-tubulin complex localization and/or behavior at non-SPB sites during interphase as well as at the end of mitosis. When we examined the colocalization of alp4-HA with mod20p in these experiments we found that the signals showed considerable, but not complete, overlap. Interestingly, apart from the SPB itself, the lack of complete overlap appeared to be due to more and/or brighter staining of mod20p relative to alp4-HA. This may suggest that if mod20p and the γ-tubulin complex are physically associated in a larger supramolecular complex, perhaps not all mod20p molecules are "loaded" with the γ-tubulin complex. Similar results were obtained when cells were costained with antibodies to mod20p and to an HA-tagged version of alp6p, another core subunit of the γ-tubulin complex [32] (data not shown).

To investigate whether mod20p might directly recruit γ-tubulin to eMTOCs and to what are likely iMTOCs, we performed coimmunoprecipitation experiments by using extracts from strains expressing native levels of Myc-tagged mod20p and HA-tagged alp4p or alp6p, expressed from their endogenous promoters. Anti-Myc antibodies coimmunoprecipitated alp4-HA and γ-tubulin,

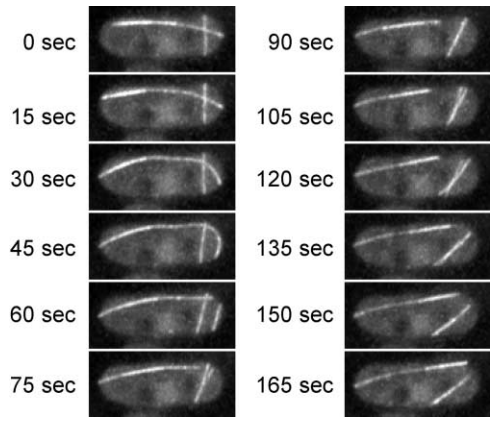

Figure 6. Bend-Breakage Microtubule Dynamics in a *mod20*Δ Cell

Time points from a deconvolved wide-field time-lapse video sequence of a *mod20*Δ cell expressing *nmt81*:GFP-atb2p, at 15 s intervals. Breakage occurs between 45 and 60 s, after which the two smaller microtubule bundles join, although their ends are still distinguishable at the 75, 105, and 120 s time points. Note that after breakage, the long microtubule bundle initially shrinks but then begins to elongate between 105 and 120 s; also note that the number of microtubules in the long bundle is not uniform along its length, and this changes over time.

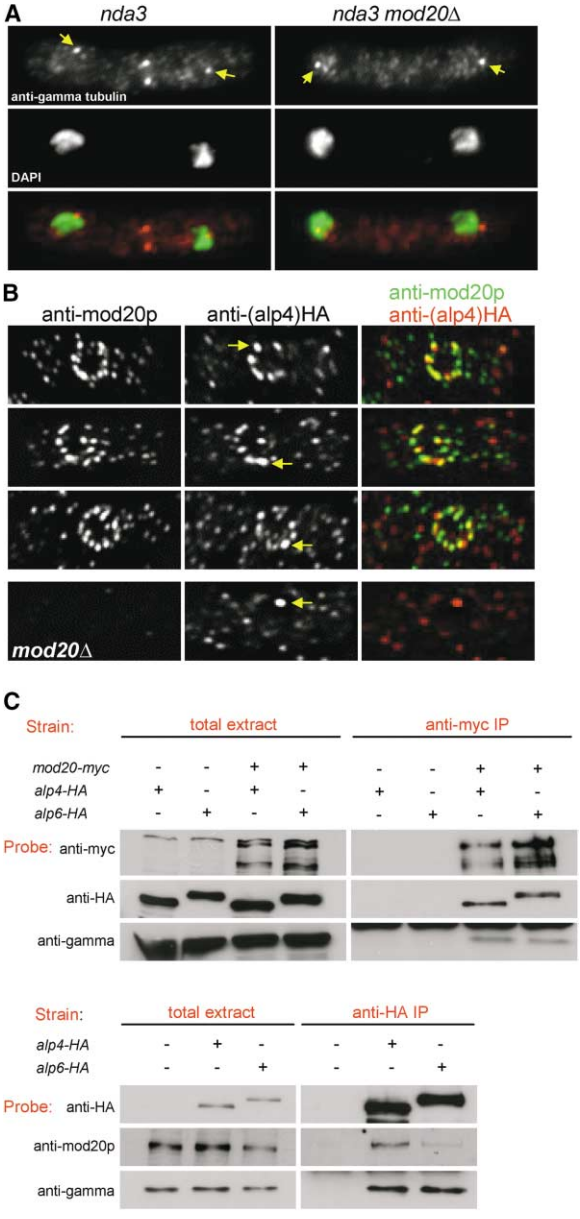

Figure 7. Mod20p Recruits the γ-Tubulin Complex to Non-Spindle Pole Body Microtubule-Organizing Centers

(A) Anti-γ tubulin (top) and DAPI (middle) staining *of nda3-km311* and *nda3-km311 mod20*Δ cells 20 min after release from mitotic metaphase arrest, when *nda3* single mutants are forming postanaphase arrays. In *mod20*Δ mutants, γ-tubulin does not relocalize to the equator but is still present at spindle pole bodies (SPBs; arrows).

(B) Anti-mod20p and anti-HA staining showing redistribution of mod20p and the γ-tubulin complex subunit alp4-HA to the nuclear surface during cold treatment (see Figure 4A). In *mod20*Δ mutants, alp4-HA does not redistribute to the nuclear surface but is still present at the SPB (arrows). Mod20p and alp4-HA show considerable overlap (yellow in merged images), although mod20p signals are greater in number and/or intensity than alp4-HA signals. Each row is a projection of three deconvolved wide-field Z sections, 0.2 um apart.

(C) Coimmunoprecipitation of alp4-HA, alp6-HA, and γ-tubulin with mod20-Myc in an anti-Myc immunoprecipitation from native cell extracts (upper panels) and coimmunoprecipitation of mod20p and γ-tubulin with either alp4-HA or alp6-HA after anti-HA immunoprecipitation (bottom panels). In all cases immunoprecipitation lanes (right) are 40× overloaded relative to total extracts (left) and are probed on the same blot; the same exposure was used for both "total extract" and "IP."

or alp6-HA and γ-tubulin, from extracts expressing mod20-Myc, but not from control extracts (Figure 7C, upper panels). To confirm these results, we also immunoprecipitated alp4-HA and alp6-HA from extracts of cells expressing untagged mod20p. mod20p was coimmunoprecipitated with alp4-HA and, to a lesser extent, alp6-HA (Figure 7C, bottom panels).

Collectively, these results indicate that mod20p physically interacts with the γ-tubulin complex in vivo. In the anti-HA immunoprecipitations (Figure 7C, bottom panel), the enrichment of alp4-HA and alp6-HA in immunoprecipitates was much greater than that of mod20p, which might suggest a low stoichiometry of mod20p association. However, in the same experiments the enrichment of alp4-HA and alp6-HA was also much greater than that of γ-tubulin itself, indicating either that there is a considerable amount of cytoplasmic alp4p and alp6p not associated with γ-tubulin in vivo or that "core" interactions between *alp* proteins and γ-tubulin are disrupted under our extraction conditions (see also [32]). Thus, our data are insufficient to allow us to determine the stoichiometry of mod20p relative to other components of the complex.

mod20-Related Proteins in Higher Eukaryotes

The amino-acid sequence of mod20p suggests that it has a globular N-terminal domain of approximately 290 amino acids, with extensive regions of α-helical coiled-coil in the remaining 825 amino acids, as predicted by PAIRCOIL [33]. Using BLAST searches, we identified related proteins in the filamentous fungus *Neurospora crassa*, as well as the *Aspergillus nidulans* protein apsB [16]. Interestingly, by using the N-terminal domain of mod20p in more refined PSI-BLAST searches [34], we were able to identify within these fungal proteins a small region of sequence similarity shared with higher eukaryotic proteins (Figure 8), including *Drosophila* centrosomin [35], a predicted zebrafish protein, and two mammalian proteins, the cyclic nucleotide phosphodiesterase binding protein PDE4DIP/myomegalin [36] and the CDK5 activator binding protein CDK5RAP2 [37]. We also found a second related fission yeast protein, pcp1p [38]. E values for these "hits" ranged between approximately 10^{-39} and 10^{-17}, with a sharp cut-off between the proteins identified and the next best "hit" (an unrelated protein; E value = 0.007). Although no related budding-yeast proteins were identified from our database searches (up to E values of 100), functional criteria led us to determine by T-COFFEE alignment [39] whether the budding-yeast SPB proteins Spc110p and Spc72p [40] contained any portion of this conserved region (see Discussion). We found a very small region of similarity between Spc110p and the proteins identified from database searches (Figure 8), but no similarity between these proteins and Spc72p (not shown). Altogether, these sequence similarities suggest that functional homologs of mod20p are likely to exist in mammalian cells (see Discussion) and may play a role in regulating MTOCs.

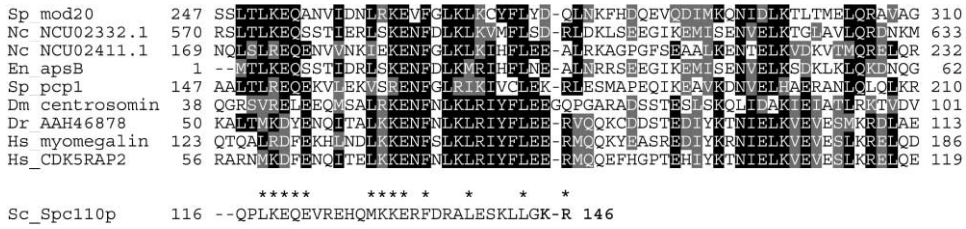

Figure 8. Alignment of a 64 Amino Acid Region of mod20p with Other Sequences from Fungi and Higher Eukaryotes

Representative examples of related proteins identified after three iterations of a PSI-BLAST search with the amino-terminus of mod20p; any other proteins identified were obvious homologs in closely related species (e.g., mouse, rat, *M. grisea*, *P. anserina*); no equivalent protein was identified in *C. elegans*. Numbers indicate amino acid residues for each individual protein, starting at the extreme amino-terminus; in all cases the region of interest is found in the amino terminus of proteins (including NCU02332, which is 2561 amino acids long). Beneath the alignment is shown a portion of the budding-yeast spindle pole body protein Spc110p, which shows very limited similarity to mod20p within this region (asterisks). However, Spc110p was not identifiable as a mod20p-related protein by PSI-BLAST searches. Accession numbers of sequences used were: *S. pombe* mod20p, NP_588284; *N. crassa* NCU02332, XP_331108; *N. crassa* NCU02411, XP_331187; *A. nidulans* apsB, CAA05918; *S. pombe* pcp1p, Q92351; *D. melanogaster* centrosomin, NP_725298; *D. rerio* unnamed protein, AAH46878; *H. sapiens* PDE4DIP/myomegalin, BAA32299; and *H. sapiens* CDK5RAP2, Q96SN8.

Discussion

We have identified a novel protein, mod20p, that plays a critical role in the nucleation and organization of essentially all fission yeast microtubule arrays apart from the mitotic spindle. In perturbation experiments, and at steady state, *mod20*Δ mutants are defective in nucleation from non-SPB MTOCs during both interphase and mitosis. In addition, *mod20*Δ mutants show only weak cytoplasmic nucleation from the SPB during interphase and are impaired in astral microtubule nucleation from the SPB during mitosis. The wild-type interphase SPB is normally inactive for microtubule nucleation, or nearly so [41]. We have not determined whether the weak interphase SPB microtubule nucleation activity seen in *mod20*Δ mutants also exists in wild-type cells or whether it occurs in *mod20*Δ cells only because there is no competition with iMTOC nucleation (see below). The localization of mod20p particles to well-characterized MTOCs in unperturbed cells, to future microtubule nucleation sites in microtubule regrowth experiments, and to different points along microtubule bundles at steady state suggests that mod20p plays a direct role in nucleation, and this is further supported by our observation that mod20p is required for the localization of, and physically interacts with, components of the γ-tubulin complex.

Is mod20p strictly involved in microtubule nucleation? During interphase, the dynamics and turnover of microtubule bundles in *mod20*Δ mutants deviate considerably from wild-type, and the number of mod20p-containing satellite particles associated with microtubules is likely to exceed the number of individual microtubules. This could suggest that mod20p has additional, as-yet-unidentified roles in regulating microtubule dynamics. However, we believe that a single defect in microtubule nucleation may be sufficient to explain the aberrant microtubule distribution and dynamics of *mod20*Δ mutants, and we argue this as follows: Immunofluorescence experiments suggest that in wild-type fission yeast at steady state, the free soluble tubulin concentration is very low, with most tubulin existing in microtubules (K.E.S., unpublished data; this is also shown in Figure 3, in which cells with disrupted microtubules have a higher "background" fluorescence because of signal from fixed soluble tubulin). Thus, in wild-type cells, dynamic microtubule plus ends will "compete" for a relatively small pool of free tubulin and undergo dynamic instability with characteristic parameters of growth, shrinkage, catastrophe and rescue [42]. By contrast, cells with a reduced capacity for microtubule nucleation, such as *mod20*Δ mutants, will tend to have fewer microtubules, and thus fewer microtubule ends, per cell, lessening competition among microtubule ends for free tubulin (which may also be increased in concentration). These conditions are likely to have considerable effects on the parameters of dynamic instability, and consequently on microtubule bundling as well. The importance of free-tubulin concentration to microtubule dynamics in a finite cell volume is underscored by results from our microtubule regrowth experiments after cold treatment in wild-type cells; during the first minute of warming, before the system reaches steady state, an initially high free-tubulin concentration (as a result of microtubule disruption due to cold treatment) drives a rapid burst of growth of many shorter microtubules, and these later convert into fewer, longer microtubules as the system approaches steady state and a lower free-tubulin concentration. Unusual interphase microtubule distributions and dynamics have previously been observed in certain γ-tubulin complex mutants in fission yeast [31, 32, 43], and we suggest that, as in *mod20*Δ mutants, these phenotypes may not be the result of the γ-tubulin complex regulating dynamics directly but rather an indirect consequence of altering the boundary conditions of a dynamic system. There may be parallels between these types of microtubule dynamics and the properties of noncentrosomal, free microtubules observed in vertebrate centrosome-free cytoplasts [44].

Given the striking microtubule nucleation defects observed in *mod20*Δ mutants both in perturbation experiments and at steady state, it may seem paradoxical that they have any interphase microtubules at all. Indirect evidence suggests that microtubules nucleated by the SPB at the end of mitosis could provide an initial source of interphase microtubules, which, over time, develop

into more complex bundles, as in our microtubule regrowth experiments (Figure 3, Suppl. Figure 2). In some *mod20*Δ cells expressing GFP-atb2p, complicated microtubule dynamics were directly observed at the end of mitosis, as microtubules grew out of the SPB or the spindle at the end of mitosis and somehow escaped the nucleus to establish an independent existence in the cytoplasm. However, because this was a relatively rare phenomenon, and separate experiments suggest that this level of GFP-tubulin expression does perturb at least some aspects of microtubule organization in *mod20*Δ mutants (but not in wild-type cells; see Table S1), we cannot be sure whether this particular behavior is truly physiological. It is also possible that in *mod20*Δ cells expressing only endogenous, untagged tubulins, there is a low level of microtubule nucleation from the interphase SPB under steady-state conditions, although have no means of detecting it.

Our observation that mod20p can coimmunoprecipitate the γ-tubulin complex components alp4p and alp6p, as well as γ-tubulin itself, suggests a mechanism in which mod20p recruits the γ-tubulin complex to non-SPB microtubule nucleation sites during both interphase and at the end of mitosis. Although we have demonstrated that mod20p is required for γ-tubulin recruitment to the eMTOC, γ-tubulin complex proteins have not yet been localized to iMTOCs in unperturbed cells [30, 31], although recent work suggests that γ-tubulin satellites may exist near the eMTOC [9]. In cold-treated interphase cells, we observed a mod20p-dependent accumulation of alp4p and alp6p at the nuclear surface, and these proteins partially colocalized with mod20p itself. Thus, although this is not formally proven, we suggest that mod20p interphase satellite particles in unperturbed cells represent iMTOCs. It is possible that at any given time, only a fraction of these satellites are associated with the γ-tubulin complex. In this light, the rapid linear movements of mod20-GFP are particularly interesting. They could represent either mod20p actively moving along microtubules or, alternatively, mod20p bound to a microtubule minus end and being moved passively by microtubule-microtubule sliding. Further work will clarify the behavior and function of these structures.

Although mod20p is required for cytoplasmic astral microtubule nucleation during mitosis and for assembly of the postanaphase array subsequent to mitosis, several lines of evidence suggest that mod20p is unlikely to play a major direct role in the assembly of the intranuclear mitotic spindle. First, in *mod20*Δ mutants the spindle itself appears morphologically normal, and in mitotic arrest-and-release experiments, *mod20*Δ mutants assemble and elongate spindles, and undergo anaphase, at the same rate as *mod20*+ cells. The lack of astral microtubules in *mod20*Δ mutants might have been expected to lead to a delay in entry to anaphase because of the spindle orientation checkpoint [45–49], but this was not observed, perhaps as a result of the lengthy metaphase arrest; this deserves closer examination in the future. Second, *mod20*Δ cells were found to be viable in combination with several spindle assembly checkpoint mutants [22], indicating that if mod20p does play a more subtle role in spindle function, its loss is insufficient to activate the spindle assembly checkpoint. However, we note that we did observe a slightly elevated minichromosome loss rate in *mod20*Δ cells relative to wild-type cells. We suggest that this could be due to a combination of more indirect effects of the *mod20*Δ mutation, such as the eccentric position of the interphase nucleus, the lack of astral microtubules, and/or the persistence of the spindle at the end of mitosis (Figures 5F and 5G). It is also possible that spindle dynamics at the very end of mitosis are altered in *mod20*Δ mutants because of a lack of competition between spindle MTOCs and the eMTOC for free tubulin, according to the arguments about competition outlined above (see, for example, Movies 6 and 7).

Why isn't mod20p required for mitotic spindle assembly? In budding yeast, the protein Spc110p promotes spindle microtubule nucleation by recruiting the γ-tubulin complex to the nucleoplasmic face of the SPB, whereas a different protein, Spc72p, promotes astral-microtubule nucleation by recruiting the γ-tubulin complex to the cytoplasmic face of the SPB [40]. Although Spc110p and Spc72p were not identified in our database searches, Spc110p did show a very weak similarity to a portion of the conserved region of mod20p. Spc72 did not, consistent with previous sequence analyses [40]. The fact that two differently localized SPB proteins, each able to recruit the γ-tubulin complex, can mediate distinct aspects of SPB microtubule nucleation in budding yeast suggests that an analogous situation may also occur in fission yeast. A plausible candidate for the mitotic-spindle SPB nucleator is the essential gene *pcp1*+ [38]. Pcp1p shows limited sequence similarity with mod20p, specifically in the region conserved with higher eukaryotes (Figure 8; see also below) and is localized to the SPB, where it may play a role in spindle assembly [38]. We suggest that spindle microtubule nucleation from the SPB in fission yeast may depend on pcp1p and that astral microtubule nucleation may depend on mod20p. It will be interesting to determine if pcp1p and mod20p reside within different domains of the SPB; an attractive hypothesis is that pcp1p resides on the nucleoplasmic face of the SPB and that mod20p resides on the cytoplasmic face. In this light it is interesting to note that during interphase in fission yeast, the SPB is not embedded in the nuclear envelope as it is in budding yeast [8]. Thus, it is possible that the very limited cytoplasmic microtubule nucleation capacity observed at the interphase SPB in *mod20*Δ mutants is actually due to pcp1p on the "nucleoplasmic" face.

Mod20p is the first protein known to play a direct role in the recruitment of γ-tubulin and microtubule-nucleating capacity to noncentrosomal MTOCs. In both filamentous fungi and higher eukaryotes, we identified several proteins containing a small region of sequence similarity to mod20p. All are large proteins (with molecular weights greater than 120 kDa), and all contain regions of predicted α-helical coiled coil to varying extents. Although we did not find comparable proteins from budding yeast in our searches, it seems plausible that the budding-yeast proteins Spc110p and Spc72p fulfill the same molecular role as mod20p-related proteins but have undergone even further sequence divergence; we note that, unlike fission yeast, budding yeast does not exhibit any non-SPB microtubule nucleation during ei-

ther mitotic or meiotic cell cycles [50]. In higher eukaryotes, we identified one related protein, centrosomin, in *Drosophila* and two distinct, little-characterized proteins in mammalian cells. Centrosomin is thought to exist in three isoforms and plays a role in microtubule nucleation and recruitment of γ-tubulin to the centrosome via an interaction with the γ-tubulin complex [51–53], although its precise function during development is still not clear [54]. Of the two mammalian proteins identified, PDE4-DIP/myomegalin is expressed in muscle cells and has been localized to pericentrosomal/Golgi regions in tissue culture cells [36]. Although it was originally isolated in a two-hybrid screen for proteins interacting with a cyclic nucleotide phosphodiesterase, its cellular function remains largely unexplored. CDK5RAP2 was also originally isolated in a two-hybrid screen, for proteins interacting with an activator of Cdk5 [37], and it is widely expressed in human tissues. A very recent proteomics analysis of the centrosome indicates that CDK5RAP2 is enriched at the centrosome [55], although its function is not known. Previous sequence analyses have suggested that budding yeast Spc110p and fission yeast pcp1p are orthologs of the mammalian protein kendrin/pericentrin [38, 56], but these analyses depended primarily on similarity in a carboxy-teminal calmodulin binding region and on regions of coiled coil, whereas the conserved region highlighted by our work is in the amino terminus of all of the proteins identified. Thus, the precise relationships among these large and likely complex proteins still remain somewhat unclear. It will be particularly interesting to determine whether PDE4-DIP/myomegalin and CDK5RAP2 play a role in centrosomal and noncentrosomal microtubule organization in differentiated and nondifferentiated cells. If they do, it may be useful to describe this family of proteins collectively as "centrosomins" to reflect a common function, even if it is not limited to the centrosome.

Experimental Procedures

Yeast Strains

Fission yeast strains were grown in EMM minimal medium or YE5S medium according to conventional procedures [57]. Gene deletion of *mod20+* and gene tagging of *mod20+* and *atb2+* were performed by PCR-mediated gene-tagging methods, as described [58]. The alp4-HA- and alp6-HA-tagged strains were generously provided by Dr. Takashi Toda (CRUK, London).

Physiological Experiments

For microtubule regrowth experiments, cultures grown in EMM minimal medium were chilled in flasks in an ice water slurry for 30 min and then returned to shaking water baths at 32°C. Samples were quickly removed from the culture and harvested by filtration, fixed in −80°C methanol, and later processed for immunofluorescence. For metaphase arrest-and-release experiments, *nda3-KM311* cells were grown in YE5S medium for 9 hr at 18°C and then shifted to shaking water baths at 36°C. Samples were taken and processed as above.

Antibodies

Anti-mod20p antibodies were raised in sheep against a GST-mod20p fusion protein. Although crude anti-mod20p antiserum produced a single band that was of the expected size on Western blots and was absent in *mod20Δ* mutants (not shown), affinity purification was required to reduce background levels for immunofluorescence. Anti-mod20p antibodies were therefore further purified against a 6xHis-mod20p fusion protein on blots. Anti-sad1p antibodies were kindly provided by Prof. Iain Hagan (Paterson Institute, Manchester, UK), and TAT1 anti-tubulin antibodies [59] were provided by Prof. Keith Gull (Oxford University). Anti-γ tubulin antibody (Sigma, clone GTU-88) was further purified from ascites fluid on protein G-agarose before use for immunofluorescence. Anti-Myc (9E10) and anti-HA antibodies (12CA5, for immunoprecipitation and Western blotting) were provided by Dr. Irina Stancheva (Edinburgh University). For immunofluorescence of HA epitopes, rat monoclonal antibody 3F10 (Roche) was used.

Immunofluorescence and Microscopy

Cells were fixed for immunofluorescence with cold (−80°C) methanol or with freshly prepared formaldehyde (3%) and processed according to standard methods [60, 61]. In some cases when very low fluorescence background was required, a different blocking solution, KOM1, was used. KOM1 contains 100 mM NaPIPES (pH 6.8), 1 mM MgCl2, 2% nonfat milk, 0.1 M lysine (monohydrochloride), 5% glycerol, and 0.05% NaN3. This was clarified twice by centrifugation and sterile-filtered before use. Secondary antibodies were AlexaFluor conjugates (Molecular Probes).

Laser-scanning confocal microscopy was used for generating the images in Figures 1D, 1E, 3A–3M, and 5. Images were collected with a Leica TCS Confocal microscope and a 100X/1.3 NA objective lens. In all cases, projections through the entire cell volume are shown. Conventional wide-field fluorescence microscopy was used for generating the images in Figures 2, 3N, and 7A. Images were collected with a Nikon TE300 microscope and a 100×/1.4NA Plan-Apo objective lens on a Photometrics CoolSnap HQ camera with Metamorph software. Deconvolved wide-field fluorescence microscopy was used for generating the images in Figures 4, 6, and 7B. Images were collected on the Nikon TE300 microscope system with the additional use of Prior filter wheels and a PiFoc piezofocus drive. Fixed-cell images were collected at 0.2 μm intervals, and live-cell images were collected at 0.6 um intervals. Images were further processed with Softworx (Applied Precision) via manufacturer-specific optical transfer functions.

Time-lapse movies were made by the same system as for deconvolution, with a Nikon "ND8" filterinserted in the light path so that photobleaching would be reduced.

Immunoprecipitations

For preparation of native cell extracts, cells were frozen in liquid nitrogen and ground to a powder with a mortar and pestle, prior to resuspension in a buffer of 50 mM NaHEPES, 75 mM KCl, 1 mM MgCl2, 1 mM EGTA, 0.5 mM DTT, 0.1% Triton X-100, and a protease inhibitor cocktail. After a clarifying centrifugation, the protein concentration was adjusted to 10 mg/ml. Six hundred microliters of each extract was incubated with 25 ul Protein A Sepharose (Amersham) for 30 min so that non-specific binding would be reduced. The supernatant from the preclearing step was then added to 25 ul Protein A Sepharose pre-loaded with 5 μg of anti-Myc antibody 9E10 or anti-HA antibody 12CA5. After incubation with rotation for 1 hr at 5°C, beads were washed six times in 1 ml of extract buffer (including TX-100) and resuspended in Laemmli sample buffer for SDS-PAGE and Western blotting..

Supplemental Data

Supplemental movies and figures are available with this article online at http://www.current-biology.com/cgi/content/full/14/9/763/DC1/.

Acknowledgments

We thank K. Gull, I. Hagan, and I. Stancheva for antibodies, K. Hardwick and T. Toda for strains, R. Allshire, W. Earnshaw, A. Merdes, and H. Ohkura for helpful discussions, and I. Samejima for testing *mod20Δ* in the *mad2Δ* background. We especially thank F. Chang for communication of results prior to publication. We also thank I. Stancheva for help with figure preparation and H. Potamus for support. K.E.S. is a Wellcome Trust Senior Research Fellow in Basic Biomedical Sciences. H.A.S. is a Caledonian Research Foundation Fellow. This work was supported by the Wellcome Trust.

Received: December 22, 2003
Revised: March 17, 2004
Accepted: March 17, 2004
Published online: March 25, 2004

References

1. Mogensen, M.M. (1999). Microtubule release and capture in epithelial cells. Biol. Cell. *91*, 331–341.
2. Keating, T.J., and Borisy, G.G. (1999). Centrosomal and non-centrosomal microtubules. Biol. Cell. *91*, 321–329.
3. Mogensen, M.M., and Tucker, J.B. (1987). Evidence for microtubule nucleation at plasma membrane-associated sites in Drosophila. J. Cell Sci. *88*, 95–107.
4. Vogl, A.W., Weis, M., and Pfeiffer, D.C. (1995). The perinuclear centriole-containing centrosome is not the major microtubule organizing center in Sertoli cells. Eur. J. Cell Biol. *66*, 165–179.
5. Mogensen, M.M., Tucker, J.B., and Baggaley, T.B. (1993). Multiple plasma membrane-associated MTOC systems in the acentrosomal cone cells of Drosophila ommatidia. Eur. J. Cell Biol. *60*, 67–75.
6. Tucker, J.B., Mogensen, M.M., Paton, C.C., Mackie, J.B., Henderson, C.G., and Leckie, L.M. (1995). Formation of two microtubule-nucleating sites which perform differently during centrosomal reorganization in a mouse cochlear epithelial cell. J. Cell Sci. *108*, 1333–1345.
7. Hagan, I.M. (1998). The fission yeast microtubule cytoskeleton. J. Cell Sci. *111*, 1603–1612.
8. Ding, R., West, R.R., Morphew, D.M., Oakley, B.R., and McIntosh, J.R. (1997). The spindle pole body of Schizosaccharomyces pombe enters and leaves the nuclear envelope as the cell cycle proceeds. Mol. Biol. Cell *8*, 1461–1479.
9. Heitz, M.J., Petersen, J., Valovin, S., and Hagan, I.M. (2001). MTOC formation during mitotic exit in fission yeast. J. Cell Sci. *114*, 4521–4532.
10. Pardo, M., and Nurse, P. (2003). Equatorial retention of the contractile actin ring by microtubules during cytokinesis. Science *300*, 1569–1574.
11. Drummond, D.R., and Cross, R.A. (2000). Dynamics of interphase microtubules in Schizosaccharomyces pombe. Curr. Biol. *10*, 766–775.
12. Tran, P.T., Marsh, L., Doye, V., Inoue, S., and Chang, F. (2001). A mechanism for nuclear positioning in fission yeast based on microtubule pushing. J. Cell Biol. *153*, 397–411.
13. Sagolla, M.J., Uzawa, S., and Cande, W.Z. (2003). Individual microtubule dynamics contribute to the function of mitotic and cytoplasmic arrays in fission yeast. J. Cell Sci. *116*, 4891–4903.
14. Snaith, H.A., and Sawin, K.E. (2003). Fission yeast mod5p regulates polarized growth through anchoring of tea1p at cell tips. Nature *423*, 647–651.
15. Sawin, K.E., and Snaith, H.A. (2004). Role of microtubules and tea1p in establishment and maintenance of fission yeast cell polarity. J. Cell Sci. *117*, 689–700.
16. Suelmann, R., Sievers, N., Galetzka, D., Robertson, L., Timberlake, W.E., and Fischer, R. (1998). Increased nuclear traffic chaos in hyphae of Aspergillus nidulans: molecular characterization of apsB and in vivo observation of nuclear behaviour. Mol. Microbiol. *30*, 831–842.
17. Mata, J., and Nurse, P. (1997). tea1 and the microtubular cytoskeleton are important for generating global spatial order within the fission yeast cell. Cell *89*, 939–949.
18. Chen, C.R., Li, Y.C., Chen, J., Hou, M.C., Papadaki, P., and Chang, E.C. (1999). Moe1, a conserved protein in Schizosaccharomyces pombe, interacts with a Ras effector, Scd1, to affect proper spindle formation. Proc. Natl. Acad. Sci. USA *96*, 517–522.
19. Hagan, I., and Yanagida, M. (1995). The product of the spindle formation gene sad1+ associates with the fission yeast spindle pole body and is essential for viability. J. Cell Biol. *129*, 1033–1047.
20. Hiraoka, Y., Toda, T., and Yanagida, M. (1984). The NDA3 gene of fission yeast encodes beta-tubulin: a cold-sensitive nda3 mutation reversibly blocks spindle formation and chromosome movement in mitosis. Cell *39*, 349–358.
21. Niwa, O., Matsumoto, T., Chikashige, Y., and Yanagida, M. (1989). Characterization of Schizosaccharomyces pombe minichromosome deletion derivatives and a functional allocation of their centromere. EMBO J. *8*, 3045–3052.
22. Millband, D.N., and Hardwick, K.G. (2002). Fission yeast Mad3p is required for Mad2p to inhibit the anaphase-promoting complex and localizes to kinetochores in a Bub1p-, Bub3p-, and Mph1p-dependent manner. Mol. Cell. Biol. *22*, 2728–2742.
23. Ding, D.Q., Chikashige, Y., Haraguchi, T., and Hiraoka, Y. (1998). Oscillatory nuclear movement in fission yeast meiotic prophase is driven by astral microtubules, as revealed by continuous observation of chromosomes and microtubules in living cells. J. Cell Sci. *111*, 701–712.
24. Yamamoto, A., West, R.R., McIntosh, J.R., and Hiraoka, Y. (1999). A cytoplasmic dynein heavy chain is required for oscillatory nuclear movement of meiotic prophase and efficient meiotic recombination in fission yeast. J. Cell Biol. *145*, 1233–1249.
25. Pidoux, A.L., Uzawa, S., Perry, P.E., Cande, W.Z., and Allshire, R.C. (2000). Live analysis of lagging chromosomes during anaphase and their effect on spindle elongation rate in fission yeast. J. Cell Sci. *113*, 4177–4191.
26. Brunner, D., and Nurse, P. (2000). CLIP170-like tip1p spatially organizes microtubular dynamics in fission yeast. Cell *102*, 695–704.
27. Gunawardane, R.N., Lizarraga, S.B., Wiese, C., Wilde, A., and Zheng, Y. (2000). gamma-Tubulin complexes and their role in microtubule nucleation. Curr. Top. Dev. Biol. *49*, 55–73.
28. Schiebel, E. (2000). gamma-tubulin complexes: binding to the centrosome, regulation and microtubule nucleation. Curr. Opin. Cell Biol. *12*, 113–118.
29. Oakley, B.R. (2000). Gamma-Tubulin. Curr. Top. Dev. Biol. *49*, 27–54.
30. Horio, T., Uzawa, S., Jung, M.K., Oakley, B.R., Tanaka, K., and Yanagida, M. (1991). The fission yeast gamma-tubulin is essential for mitosis and is localized at microtubule organizing centers. J. Cell Sci. *99*, 693–700.
31. Paluh, J.L., Nogales, E., Oakley, B.R., McDonald, K., Pidoux, A.L., and Cande, W.Z. (2000). A mutation in gamma-tubulin alters microtubule dynamics and organization and is synthetically lethal with the kinesin-like protein pkl1p. Mol. Biol. Cell *11*, 1225–1239.
32. Vardy, L., and Toda, T. (2000). The fission yeast gamma-tubulin complex is required in G(1) phase and is a component of the spindle assembly checkpoint. EMBO J. *19*, 6098–6111.
33. Berger, B., Wilson, D.B., Wolf, E., Tonchev, T., Milla, M., and Kim, P.S. (1995). Predicting coiled coils by use of pairwise residue correlations. Proc. Natl. Acad. Sci. USA *92*, 8259–8263.
34. Altschul, S.F., Madden, T.L., Schaffer, A.A., Zhang, J., Zhang, Z., Miller, W., and Lipman, D.J. (1997). Gapped BLAST and PSI-BLAST: a new generation of protein database search programs. Nucleic Acids Res. *25*, 3389–3402.
35. Heuer, J.G., Li, K., and Kaufman, T.C. (1995). The Drosophila homeotic target gene centrosomin (cnn) encodes a novel centrosomal protein with leucine zippers and maps to a genomic region required for midgut morphogenesis. Development *121*, 3861–3876.
36. Verde, I., Pahlke, G., Salanova, M., Zhang, G., Wang, S., Coletti, D., Onuffer, J., Jin, S.L., and Conti, M. (2001). Myomegalin is a novel protein of the golgi/centrosome that interacts with a cyclic nucleotide phosphodiesterase. J. Biol. Chem. *276*, 11189–11198.
37. Ching, Y.P., Qi, Z., and Wang, J.H. (2000). Cloning of three novel neuronal Cdk5 activator binding proteins. Gene *242*, 285–294.
38. Flory, M.R., Morphew, M., Joseph, J.D., Means, A.R., and Davis, T.N. (2002). Pcp1p, an Spc110p-related calmodulin target at the centrosome of the fission yeast Schizosaccharomyces pombe. Cell Growth Differ. *13*, 47–58.
39. Notredame, C., Higgins, D.G., and Heringa, J. (2000). T-Coffee: a novel method for fast and accurate multiple sequence alignment. J. Mol. Biol. *302*, 205–217.
40. Knop, M., and Schiebel, E. (1998). Receptors determine the cellular localization of a gamma-tubulin complex and thereby the site of microtubule formation. EMBO J. *17*, 3952–3967.
41. Masuda, H., Sevik, M., and Cande, W.Z. (1992). In vitro microtu-

bule-nucleating activity of spindle pole bodies in fission yeast Schizosaccharomyces pombe: cell cycle-dependent activation in xenopus cell-free extracts. J. Cell Biol. *117*, 1055–1066.
42. Desai, A., and Mitchison, T.J. (1997). Microtubule polymerization dynamics. Annu. Rev. Cell Dev. Biol. *13*, 83–117.
43. Fujita, A., Vardy, L., Garcia, M.A., and Toda, T. (2002). A fourth component of the fission yeast gamma-tubulin complex, Alp16, is required for cytoplasmic microtubule integrity and becomes indispensable when gamma-tubulin function is compromised. Mol. Biol. Cell *13*, 2360–2373.
44. Borisy, G.G., and Rodionov, V.I. (1999). Lessons from the melanophore. FASEB J. *13* (*Suppl 2*), S221–S224.
45. Gachet, Y., Tournier, S., Millar, J.B., and Hyams, J.S. (2004). Mechanism controlling perpendicular alignment of the spindle to the axis of cell division in fission yeast. EMBO J. Published online March 11, 2004. 10.1038/sj.emboj.7600156.
46. Gachet, Y., Tournier, S., Millar, J.B., and Hyams, J.S. (2001). A MAP kinase-dependent actin checkpoint ensures proper spindle orientation in fission yeast. Nature *412*, 352–355.
47. Rajagopalan, S., Bimbo, A., Balasubramanian, M.K., and Oliferenko, S. (2004). A potential tension-sensing mechanism that ensures timely anaphase onset upon metaphase spindle orientation. Curr. Biol. *14*, 69–74.
48. Oliferenko, S., and Balasubramanian, M.K. (2002). Astral microtubules monitor metaphase spindle alignment in fission yeast. Nat. Cell Biol. *4*, 816–820.
49. Sato, M., Koonrugsa, N., Toda, T., Vardy, L., Tournier, S., Millar, J.B. (2003). Deletion of Mia1/Alp7 activates Mad2-dependent spindle assembly checkpoint in fission yeast. Nat. Cell Biol. *5*, 764–766; author reply 766.
50. Botstein, D., Amberg, D., Mulholland, D., Huffaker, T., Adams, A., Drubin, D., and Stearns, T. (1997). The yeast cytoskeleton. In: The Molecular and Cellular Biology of the Yeast Saccharomyces, vol. 3, J.R. Pringle, J.R. Broach, and E.W. Jones, Eds. (Cold Spring Harbor, NY: Cold Spring Harbor Laboratory Press), 1–90.
51. Megraw, T.L., Li, K., Kao, L.R., and Kaufman, T.C. (1999). The centrosomin protein is required for centrosome assembly and function during cleavage in Drosophila. Development *126*, 2829–2839.
52. Vaizel-Ohayon, D., and Schejter, E.D. (1999). Mutations in centrosomin reveal requirements for centrosomal function during early Drosophila embryogenesis. Curr. Biol. *9*, 889–898.
53. Terada, Y., Uetake, Y., and Kuriyama, R. (2003). Interaction of Aurora-A and centrosomin at the microtubule-nucleating site in Drosophila and mammalian cells. J. Cell Biol. *162*, 757–763.
54. Megraw, T.L., Kao, L.R., and Kaufman, T.C. (2001). Zygotic development without functional mitotic centrosomes. Curr. Biol. *11*, 116–120.
55. Andersen, J.S., Wilkinson, C.J., Mayor, T., Mortensen, P., Nigg, E.A., and Mann, M. (2003). Proteomic characterization of the human centrosome by protein correlation profiling. Nature *426*, 570–574.
56. Flory, M.R., Moser, M.J., Monnat, R.J., Jr., and Davis, T.N. (2000). Identification of a human centrosomal calmodulin-binding protein that shares homology with pericentrin. Proc. Natl. Acad. Sci. USA *97*, 5919–5923.
57. Moreno, S., Klar, A., and Nurse, P. (1991). Molecular analysis of the fission yeast *Schizosaccharomyces pombe*. Methods Enzymol. *194*, 795–823.
58. Bahler, J., Wu, J.Q., Longtine, M.S., Shah, N.G., McKenzie, A., 3rd, Steever, A.B., Wach, A., Philippsen, P., and Pringle, J.R. (1998). Heterologous modules for efficient and versatile PCR-based gene targeting in Schizosaccharomyces pombe. Yeast *14*, 943–951.
59. Woods, A., Sherwin, T., Sasse, R., MacRae, T.H., Baines, A.J., and Gull, K. (1989). Definition of individual components within the cytoskeleton of *Trypanosoma brucei* by a library of monoclonal antibodies. J. Cell Sci. *93*, 491–500.
60. Hagan, I.M., and Hyams, J.S. (1988). The use of cell division cycle mutants to investigate the control of microtubule distribution in the fission yeast Schizosaccharomyces pombe. J. Cell Sci. *89*, 343–357.
61. Sawin, K.E., and Nurse, P. (1998). Regulation of cell polarity by microtubules in fission yeast. J. Cell Biol. *142*, 457–471.

Note Added in Proof

Independent work from the laboratory of K. Gould has identified a gamma-tubulin complex-associated protein, mbo1p, which is identical to mod20p (Venkatram et al. Mol. Biol. Cell, in press). Their results are largely in agreement with our own.